THERMODYNAMIC ANALYSIS AND OPTIMIZATION DESIGN OF COOLING PLATE WITH MULTIPLE CHANNELS FOR LINEAR SYNCHRONOUS MOTOR

by

Fan DU [a,c*], ***Bo YANG*** [b,c], ***and Tangjia ZHANG*** [d]

[a] School of Mechanical Engineering, Southwest Petroleum University, Chengdu, China
[b] School of Mechanical Engineering, Southwest Jiaotong University, Chengdu, China
[c] Hope College, Southwest Jiaotong University, Chengdu, China
[d] School of Mechanical Engineering, Xi'an Jiaotong University, Xi'an, China

Original scientific paper
https://doi.org/10.2298/TSCI221111053D

A liquid cooling plate structure with multiple channels is proposed for linear synchronous motor in this paper. Firstly, a conjugate heat dissipation model is established, and coupling analysis with fluid and temperature fields is performed by finite volume method with different channel numbers and section shapes. The simulation results show that, the cooling capacity of proposed cooling plate is observably improved, especially for 6 channels cooling plate with elliptical section. Afterwards, adopting boundary optimization by quadratic approximation algorithm, the section dimensions of 6 channels plate with elliptical section are further optimized to realize a trade-off with heat transfer coefficient and pump power. The optimized scheme can improve heat transfer coefficient by 33.03% and reduce the pressure drop by 85.37% compared with original scheme.

Key words: *linear synchronous motor, cooling plate, multi-objective optimization, multiple channels, thermal-fluid coupling analysis*

Introduction

As a contactless electromagnetic actuator, linear synchronous motor (LSM) has the advantages of high operating efficiency, high energy density and fast control response [1], which has been widely used in rail transit, electromagnetic ejection, precision manufacture and other frontier domains. When the primary produces a traveling wave magnetic field along the running direction, electromagnetic energy will be converted into mechanical energy and heat energy with the magnetic field as the medium between the armature windings and magnets. Among them, the mechanical energy drives the LSM to operate on the established track, while the heat energy causes the temperature rise of LSM. Supposing that the temperature exceeds the safety threshold, the failure risk of windings or magnets will rapidly rise [2]. Therefore, reasonable cooling structure design plays a critical role for the output stability and operation safety of LSM.

At present, the cooling ways of motor can be divided into air-cooling [3], water-cooling [4], and oil-cooling [5]. However, due to the special topological configuration of LSM, it is difficult to install integrated air-cooling device applied to rotating motors. In contrast, liquid-cooling channels can make full use of the structural characteristics of LSM and the cooling

* Corresponding author, e-mail: jixiedufan@163.com

effect is better, so liquid-cooling has become a common choice for LSM [6]. For this type cooling structure, scholars from all over the world have carried out substantial researches and analyses.

Pei *et al.* [7] arranged a serpentine channel in water-cooling plate between the double-layers primary windings, significantly reducing the temperature rise of winding and increasing the thrust of LSM. Pan *et al.* [8] installed two bidirectional channel water-cooling plates on the upper and lower sides of the winding, respectively, to inhibit temperature rise on the primary side. Furthermore, a water-cooling channel embedded in the top of back iron was designed to increase the thrust density by Lu *et al.* [9]. Although the existing cooling plate structures can further reduce the temperature rise of LSM, the cooling channel is mostly considered as serpentine structure, and its systematic design process is rarely reflected in these researches. It means that the cooling plate still has large space in optimization design for trade-off between the cooling efficiency and manufacturing difficulty.

In contrast, with regard to the industrial domains, electronic components and lithium battery will produce higher unit heat than LSM in the process of operation, thus its radiator structure will have higher heat dissipation performance, which provides a reliable reference [10] for the cooling plate design of LSM. Zehforoosh *et al.* [11] proposed a porous channels cooling plate to enhance laminar flowforced convection, reducing the pressure drop required for the cooling of the electronics and ensuring the heat transfer capacity. Hajmohammadi *et al.* [12] utilized multiple channels filled with porous channels in conventional micro-channel radiator, improving cooling performance to over 40% .

Combined with the aforementioned structures of cooling channel, a multiple channels cooling plate is designed on the basis of existing cooling structure of permanent magnet LSM [7] to promote cooling ability in this paper. Meanwhile, the influence of design variables on heat dissipation effect and pumping power is discussed including shape and number of channels. Finally, with the pumping power and the heat dissipation effect as the optimization goals, multi-objective optimization design of the channel section structure is realized based on the boundary optimization by quadratic approximation (BOBYQA) algorithm. The optimization results can provide a basis for the cooling plate design of LSM.

Permanent magnet linear synchronous motor and cooling plate structure

The 3-D diagrammatic sketch of the permanent magnet LSM is shown in fig. 1(a), composed of coils, permanent magnets, cooling plate, and back iron [7]. The permanent magnets as the secondary are symmetrically arranged on the upper and lower sides of coils and mounted on the back iron provide the excitation magnetic field, while the coils are attached to both sides of the cooling plate to generate the interaction with permanent magnets via injecting three-phases AC current, as displayed in fig. 1(b). To dissipate the heat generated via LSM, the original cooling plate interior is processed into a serpentine channel with circular section, using a water pump to supply cooling water to take away the heat transmitted to the cooling plate surface in fig. 2. The relevant structure parameters are shown

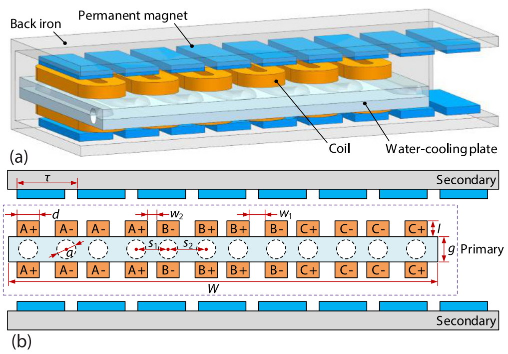

Figure 1. Permanent magnet LSM; (a) 3-D diagram and (b) topology structure

in tab. 1. Furthermore, the cooling plate material and corresponding physical parameters are shown in tab. 2.

Table 1. Structure parameters of permanent magnet LSM and original cooling plate [7]

Parameters	Values
Coil height, l	5 mm
Unilateral width of coil, d	7 mm
Adjacent distance of coils, w_1/w_2	5 mm/3 mm
Effective length of coil, h_1	40 mm
Number of coil, n	12
Resistance of coil, R	3 Ω
Equivalent current of coil, I_0	1.1 A
Cooling plate thickness, g	8 mm
Cooling plate height, H	82 mm
Cooling plate width, W	135 mm
Channel diameter, a	6 mm
Channel length, h_2	52 mm
Water inlet height, h_3	4 mm
Channel bending radius, r	4 mm
Adjacent distance of channels, s_1/s_2	10 mm/12 mm

Table 2. Cooling plate material and corresponding physical parameters

Cooling plate material	Physical parameters	Value	Unit
Aluminum	Constant pressure heat capacity	900	[$Jkg^{-1}K^{-1}$]
	Coefficient of thermal conductivity	238	[$Wm^{-1}K^{-1}$]
	Density	2700	[kgm^{-3}]
	Relative permeability	1	[1]
	Conductivity of electricity	$3.774 \cdot 10^7$	[Sm^{-1}]
	Relative dielectric constant	1	[1]
	Coefficient of thermal expansion	$23 \cdot 10^{-6}$	[K^{-1}]
	Young's modulus	$70 \cdot 10^9$	[Pa]
	Poisson's ratio	0.33	[1]
	Elastic modulus of the third order	$-2.5 \cdot 10^{11}$	[Nm^{-2}]

In order to further improve the heat dissipation capacity of the cooling plate, a multiple cooling channels is designed referring to the initial structure parameters, as exhibited in fig. 3. Compared with single channel, the advantage of multiple channels lies in the heat dissipation effect is more uniform, and the temperature difference among the coils can be effectively reduced. The heat emitted from LSM will be transmitted the wall are of channels through the contact surface among the coils and cooling plate, and discharged by the cooling liquid in the channel.

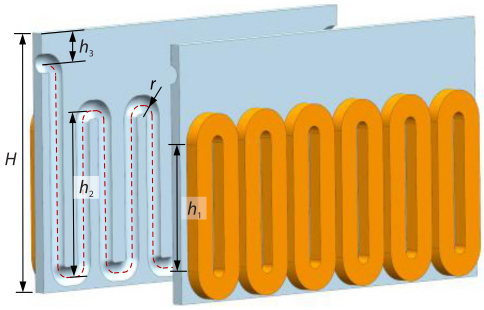

Figure 2. Original cooling plate structure

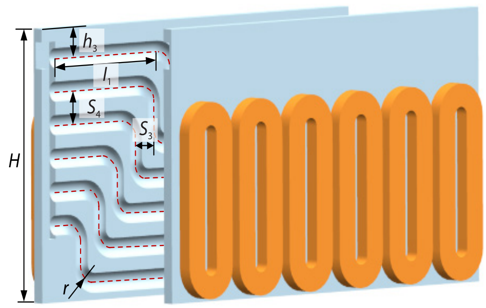

Figure 3. Proposed cooling plate structure

Notably, since the radiant heat from the permanent magnet is transferred through air to the cooling plate, whose value is minor. Therefore, the coil copper loss is considered as the only heat source transmitted to the cooling plate in this paper, and the calculation expression is:

$$P_{\mathrm{Cu}} = nI_0^2 R \tag{1}$$

where P_{Cu} is total copper loss of coils, n – the number of coils, I_0 – the equivalent phase current of coil, and R – the resistance of coil.

Furthermore, the heat flux acting on the cooling plate surface can be obtained:

$$q_w = \frac{P_{\mathrm{Cu}}}{S} \tag{2}$$

where q_w is heat flux and S – the total contact area of the coils with cooling plate.

Combined with the parameters of permanent magnet LSM in tab. 1, the total copper loss of LSM is 43.56 W and the heat flux is 0.441 W/cm^2.

Thermodynamic modelling and analysis

Conjugate heat transfer model of multiple channels cooling plate

Before solving aforementioned physical model numerically, the following assumptions are made:

- The fluid is incompressible and the laminar flow is stable.
- The thermophysical properties are constant within the operating temperature range and the effects of gravity and radiation on the heat transfer and flow can be ignored.
- The effect of viscous dissipation of fluid-flow on heat transfer is ignored.
- The physical property parameters of the liquid and solid are constant and the ambient temperature is constant.

Based on the previous assumptions and analysis, the coolant flow and energy transfer equations are:

- Fluid mass conservation

$$\frac{\partial \rho_f}{\partial t} + \nabla\left(\rho_f \vec{\mathrm{V}}\right) = 0 \tag{3}$$

- Conservation of fluid momentum:

$$\frac{\partial \rho_f}{\partial t}\vec{\mathrm{V}} + \nabla\left(\rho_f \vec{\mathrm{V}}\right)\vec{\mathrm{V}} = \nabla P \tag{4}$$

- Fluid energy conservation:

$$\rho_f c_f \frac{\partial T}{\partial t} + \nabla\left(\rho_f c_f \vec{\mathrm{V}} T\right) = \nabla\left(k_f \nabla T\right) \tag{5}$$

– Energy conservation equation for cooling plate:

$$\rho_c c_{p,c} \frac{\partial T}{\partial t} = \nabla \left(k_c \nabla T \right) \tag{6}$$

where ρ_f is the coolant density, $\vec{V}$ – the coolant velocity vector, P – the pressure, C_f – the coolant heat capacity, $c_{p,c}$ – the cooling plate heat capacity, T – the temperature, k_f – the coolant heat transfer coefficient, and k_c – the heat transfer coefficient of the cooling plate.

The boundary conditions are:

– Entrance: when $x = 0$, $u = u_{\text{in}}$, $T = T_{\text{in}}$
– Export: when $x = W$, $P = P_{\text{out}}$
– Solid-liquid interface

$$\vec{V} = 0, \ \ T_f = T_c, \ -k_f \nabla T_f \big|_n = -k_c \nabla T_c \big|_n \tag{7}$$

where P_{out} is the outlet pressure, T_f and T_c are the temperatures of the coolant and cooling plate, respectively, and n – the normal unit vector.

– Contact surface with winding

$$q_w = -k_c \nabla T_c \big|_n \tag{8}$$

– Other insulation layers

$$-k_s \nabla T_s \big|_n = 0 \tag{9}$$

When solving the fluid domain, the inlet velocity is 0.3 m/s, and the uniform temperature at the inlet of the channel is assumed to be 293 K, with constant outlet pressure and no slip on the solid wall.

The top and bottom surfaces are insulated and the heat flux q_w= 0.441 W/cm^2 loaded on the bottom surface of the cooling plate. Other parameters used to evaluate the thermal performance of the water-cooling channel can be described [13]:

– Reynolds number

$$\text{Re} = \frac{\rho_f u_{\text{in}} D_h}{\mu_f} \tag{10}$$

– Pump power

$$\Omega = \dot{Q} \Delta P = u_{\text{in}} s_f \Delta P \tag{11}$$

– Average heat transfer coefficient of water channels

$$h_m = \frac{q_w}{\overline{T}_w - T_{\text{in}}} \tag{12}$$

– Nusselt number

$$\text{Nu}_m = \frac{h_m D_h}{k_f} \tag{13}$$

– Thermal resistance：

$$R_T = \frac{T_{w,\max} - T_{\text{in}}}{q_w A} \tag{14}$$

where μ_f is the coolant viscosity, D_h – the channel diameter, $\dot{Q}$ – the volume flow rate of the channel, T_{in} – the inlet temperaturem, T_w – the average cooling channel wall temperature, $T_{w,\max}$ – the maximum wall temperature of cooling channel, and A – the surface area of bottom surface. To determine the improvement of new design in terms of heat transfer and pump power compared to the original design, a quality factor (FOM) is defined to compare the two different designs. It is described [14]:

$$\text{FOM} = \frac{\dfrac{h_{m,\text{new}}}{h_{m,\text{base}}}}{\left(\dfrac{\Omega_\text{new}}{\Omega_\text{base}}\right)^{1/3}} \tag{15}$$

where $h_{m,\text{new}}$, $h_{m,\text{base}}$ are heat transfer coefficient of the new design and the baseline design, respectively and Ω_new, Ω_base are pumping power of the new design and the baseline design, respectively.

Based on obtained key parameters, the thermal properties of cooling plates will be deeply compared and analyzed in the next subsection.

Thermodynamic analysis

The corresponding 3-D model is imported in COMSOL Multiphysics software according to the aforementioned parameters, and some basic steps (including parameter definition, material selection, physical field loading and study term settings) are performed.

To appraise the mesh division effect on the accuracy and computation time, the mesh independency analysis is firstly carried out. Thereinto, the predefined mesh division in COMSOL software is used, in which the mesh division can be divided into seven levels according to maximum mesh size, as shown tab. 3. Furthermore, the performance parameters (pressure drop and heat transfer coefficient) of cooling plates are compared in different mesh division levels by taking the original plate and proposed plate (6 channels with circle section) as examples, as displayed in fig. 4.

Table 3. Relationship between the mesh division level and maximum mesh size

Mesh division level	Maximum mesh size
Super refined	4.73 mm
More refined	7.43 mm
Refined	10.8 mm
Conventional	13.5 mm
Coarse	20.3 mm
More coarse	25.7 mm
Super coarse	40.5 mm

It can be observed from fig. 4 that, the pressure drop and heat transfer coefficient of original and proposed plate both asymptotically converge on constant values with the decrease of maximum mesh size, meaning that the model calculation accuracy will be independent on mesh when maximum mesh size is less than a certain value. By contrast, the running time augments exponentially with maximum mesh size reducing. Therefore, considering the balance among the calculation accuracy and running time, we finally selected the maximum mesh size of 7.43 mm as the criterion for mesh division in the following works.

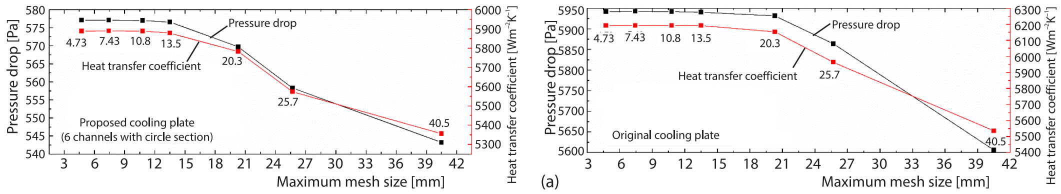

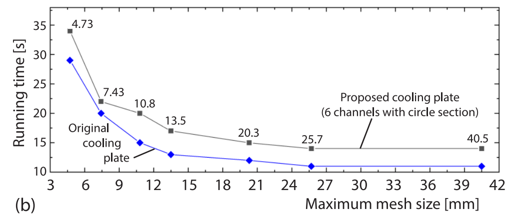

Figure 4. Comparison of performance parameters of cooling plates in different mesh sizes; (a) pressure drop and heat transfer coefficient and (b) running time

Based on the analysis presented previously, the cooling plate structure in fig. 2 is used as the baseline and simulated under the initial flow velocity of 0.3 m/s. Its temperature distribution cloud is shown in fig. 5. According to fig. 5, it can be found that its maximum temperature in coils is 303 K, which is the same as that reported in [7], while its pressure drop and heat transfer coefficient can be obtained as 5942 Pa and 6192.3 W/m²K, respectively, so its performance parameters can be used as a reference and substituted into the FOM.

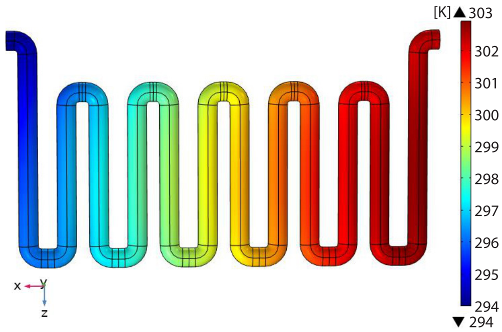

Figure 5. Baseline temperature distribution cloud diagram of cooling plate structure

Furthermore, to investigate the effects of section shapes and number of channels on the heat dissipation effect for proposed cooling plate, comparative analyses were conducted for cooling channel structures with different section shapes and number. Among them, the analyzed section shapes mainly include five categories: circle, ellipse, square, rectangle, and rounded rectangle, as shown in fig. 6, where the corresponding section dimensions are shown in tab. 4. The number of channels is selected as 2-6, and the channel distance is divided equally according to the shape. Moreover, the structural parameters of the initial scheme of proposed cooling plate are shown in tab. 5, and the initial coolant flow rate is set to 0.3 m/s, while all other initial conditions are identical. On the basis of the structure, the finite element models were established to analyze the thermal property of coils and cooling plate, as displayed in fig. 7.

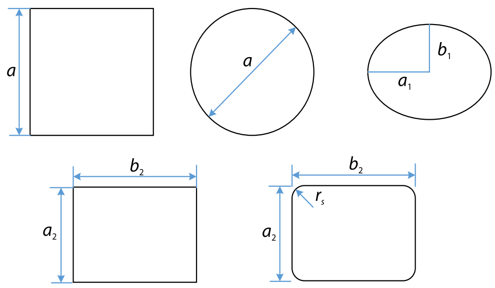

Figure 6. Cooling channel section shapes

Table 4. Section sizes of different section

Section size signal	Value [mm]
a	6
a_1	2
b_1	3
a_2	4
b_2	6
r_s	1

Table 5. Structural parameters of proposed cooling plate

Parameter	Value
Thickness of the pipes, *g*	8 mm
Height of cooling plate, *H*	82 mm
Width of Cooling plate, *W*	135 mm
Diameter of cold pipe, *a*	6 mm
The distance between the cold pipe and the end face of the cooling plate, h_3	4 mm
Length of cold tube at the top, l_1	45 mm
Cold pipe bending rounded, *r*	6 mm
Cold pipe center vertical adjacent spacing, s_3	10 mm
Center horizontal spacing of cold pipe, s_4	8 mm

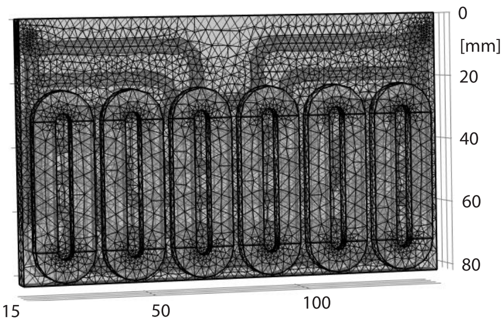

Figure 7. Finite element model of thermal analysis of motor coils and cooling plate

Moreover, fig. 8 shows the comparison of the pressure drop, heat transfer coefficient and FOM under different section shapes and channel number. By analyzing fig. 8(a), it can be found that among the five section shapes of the cooling plate structure, the pressure drop of rectangle section cooling plate with different number of channels is always the lowest, followed by square section. When the channels number is 2, the pressure drop of all section shapes of cooling plate is the highest. With the number of cooling plate increases, the pressure drop basically shows a decreasing trend. Among them, ellipse and rounded rectangle section have the most obvious decreasing trend, indicating that pressure drop will be reduced with increasing of channels number.

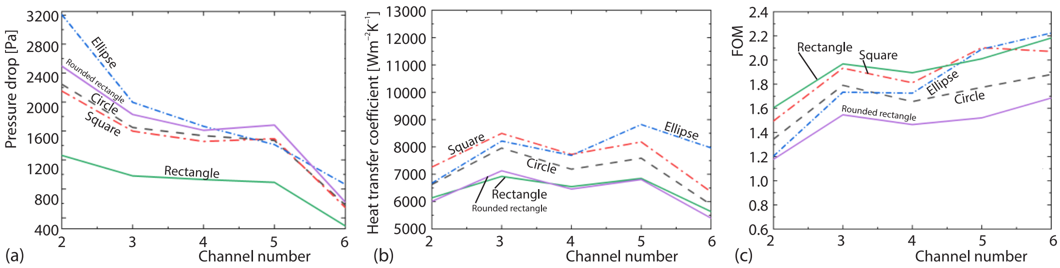

Figure 8. Comparison for different section shapes and number of channels; (a) pressure drop, (b) heat transfer coefficients, and (c) FOM

As can be seen from fig. 8(b), the heat transfer coefficient is higher when the channels number is 3 or 5, in which the ellipse section cooling plate has the highest heat transfer coefficient when the channel number is 5. Figure 8(c) displays that among all cooling plates with diverse sections, where cooling channels with rectangle and ellipse section have higher FOM values, and when the channel number is 6, all section cooling plates have higher FOM, for the ellipse section that reaches the largest FOM of 2.22. The aforementioned analysis shows that it can achieve better overall thermal performance compared with original structure [7] since all of the FOM values are greater than 1. Especially for the 6 channel cooling plate, which has the best thermal performance. Therefore, the coolant and coil surface temperatures under the 6 channels of each section shape cooling plate are further analyzed, and the temperature distribution maps are shown in fig. 9. The simulation results show that among the five types of section shapes in the cooling channel, the rectangle and ellipse section have the lower maximum temperature. Thus, it is necessary to conduct comparative analysis of the thermal performance for these two section shapes.

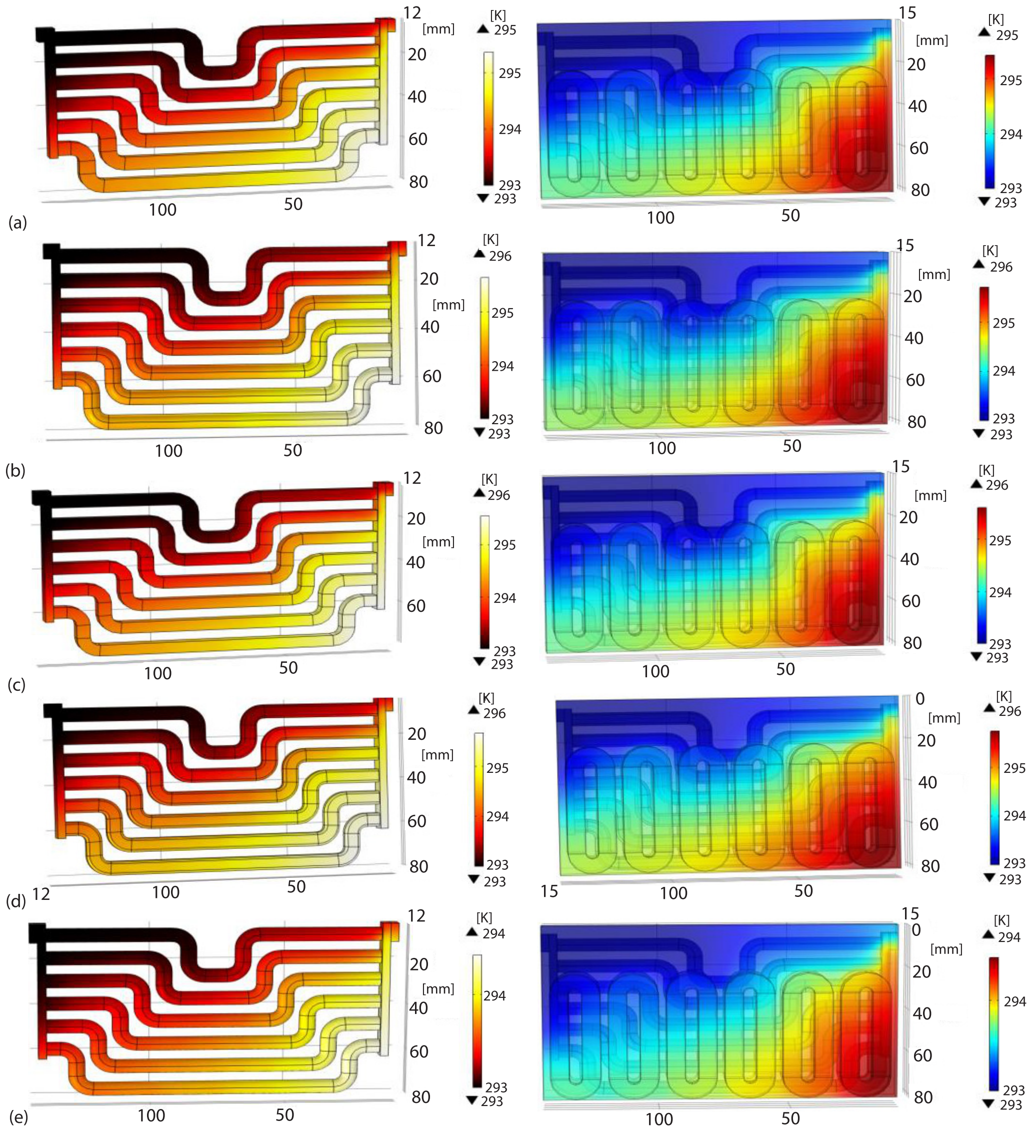

Figure 9. Surface temperature distribution map of coolant and coils of 6 channels cooling plate structure with different section shape; (a) rectangle section, (b) circular section, (c) square section, (d) rounded rectangular section, and (e) elliptical section

In fact, the section area is also the main factor affecting the cooling effect. Since the pressure drop is related to the pump power, where the higher the pressure drop, the higher the required pump power. Thus, in order to obtain the integrated optimal pressure drop and heat transfer coefficient, simulations were performed for the cooling plate structure with 6 channels elliptical and rectangular section by changing the length of the rectangular sides and the *a*-axis and axes *b*-axis length of the ellipse to analyze key indicators, including the pressure drop, heat transfer coefficient, Reynolds and Nussle numbers. While using the quality coefficients FOM to compare the related designs, and the simulation analysis results are shown in the figs. 10 and 11.

As shown in figs. 10(a)-10(c), with the increase of axes length, the pressure drop and heat transfer coefficient of the cooling plate structure with 6 channels ellipse section decrease continuously, and its Reynolds number increases continuously. While Nusselt number increases first and then decreases, its FOM also increases first and then decreases where the turning point of Nusselt number and FOM are both ($a_1 = 2$ mm, $b_1 = 3$ mm), and the largest FOM in this case is 2.22. As shown in fig. 11(a)-11(c), with the rise of side length, the pressure drop of the cooling plate structure with 6 channels rectangle section decreases continuously, but the heat transfer coefficient increases continuously. The Reynolds and Nusselt numbers are increasing, while the FOM is also decreasing. When the width of the rectangle is 4 mm and the length is 6 mm, the FOM is the largest, which is 2.18.

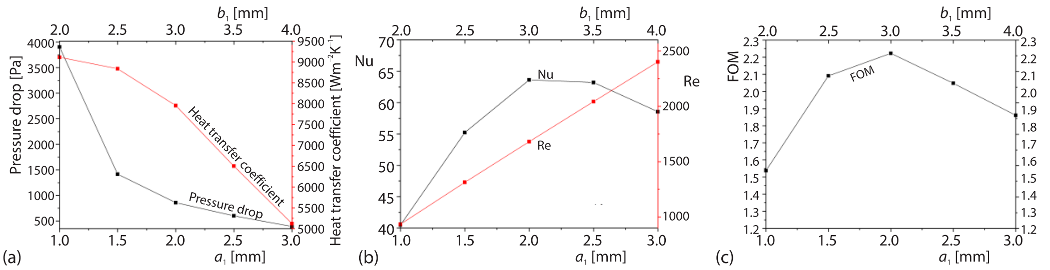

Figure 10. Comparison of structural performance parameters of cooling plate with 6 channels ellipse section; (a) pressure drop and heat transfer coefficient, (b) Nusselt and Reynolds numbers, and (c) FOM

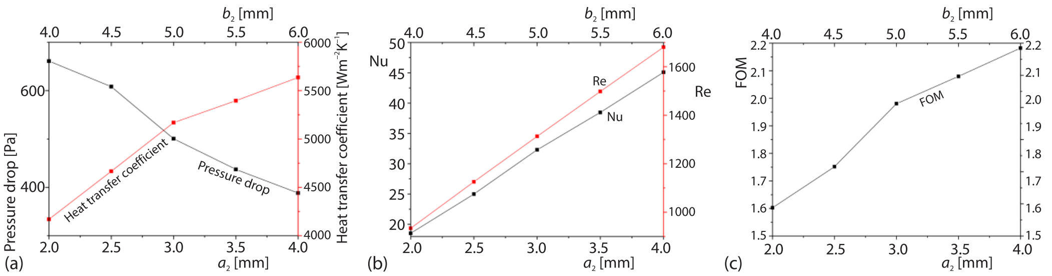

Figure 11. Comparison of structural performance parameters of cooling plate with 6 channels rectangle section; (a) pressure drop and heat transfer coefficient, (b) Nusselt and Reynolds numbers, and (c) FOM

Through the aforementioned analysis, it can be summarized that the comprehensive heat dissipation performance of the ellipse section cooling plate is better than that of the rectangle section. Although the better section size of cooling channel can be determined from the analysis in figs. 10 and 11, the optimal outcome still needs to be explored due to the simulation here is actually used in the way of parameter scanning and the FOM changes are not actually fully increasing or decreasing. In next section, resorting to BOBYQA algorithm, multi-objective optimization design of proposed cooling plate with ellipse section is further carried out, to realize a trade-off with heat transfer coefficient and pump power.

Multi-objective optimization design of multiple channels water-cooling structure

In the performance analysis of the cooling plate with multiple channels, the optimal values of the section dimensions were found by parametric studies. To further obtain the optimal section size, the BOBYQA algorithm is adopted to replace the parametric scan. Thus, heat transfer coefficient and pump power can be used as a measure of heat dissipation performance, *i.e.*, it is used as objective functions, and the optimization goals are to find the maximum heat transfer coefficient as well as minimum pressure drop.

For BOBYQA, it is an optimization algorithm proposed by Powell [15] for complex objective function problems that does not require the computation of the derivative of the objective function. The algorithm replaces the objective function with a quadratic approximation function during each iteration of the computation, and the interpolation points can be automatically selected and adjusted. In this way, the BOBYQA optimization algorithm can effectively solve highdimensional optimization problems with high solution efficiency.

Consequently, the BOBYQA algorithm is used to simulate the 6 channel cooling plate structure with ellipse section considering different section dimensions, in which the water flow rate and heat flux of coils are used as constraints. To compare the performance of the two structures with different section dimensions, the average pressure drop and average heat transfer coefficient are reanalyzed. Thus, the optimization variables are the *a*-axis length and *b*-axis length, and the optimization objectives are the maximum heat transfer coefficient and minimum pressure drop. According to the analysis results in fig. 10, the ellipse *a*-axis length of 2 mm and baxis length of 3 mm are taken as the initial points, and the *a*-axis length is taken in the range of 1 mm and 3 mm, and the *b*-axis length is taken in the range of 2 mm and 4 mm. Table 6 shows the correspondence between the *a*-axis and *b*-axis lengths and the targets in the BOBYQA iterative optimization process.

Table 6. The BOBYQA iteration process

	Control variables		Optimization objectives		Objective function
Iterations	a_1 [mm]	b_1 [mm]	Heat transfer coefficient [$Wm^{-2}K^{-1}$]	Pressure drop [Pa]	FOM
1	2	3	7963.4	862.14	2.2236
2	2.2	3	7584	808.03	2.1639
3	2	3.2	7863.1	813.37	2.2387
4	1.8	3	8296.3	955.39	2.2412
5	2	2.8	8237.4	896.3	2.2705
6	1.8293	2	8613.4	1323.3	2.0850
7	2	2.8	8237.4	896.3	2.2705

It can be seen from tab. 6 that the FOM is maximum at 2.2705, when the length of the *a*-axis is 2 mm and the length of the *b*-axis is 2.8 mm. Accordingly, the pressure drop is 896.3 Pa and heat transfer coefficient is 8237.4 W/m²K, respectively. The optimized results are compared with those after another parametric scan (scaled to 0.2 mm) were compared with the results after another parametric scan (scaled to 0.2 mm), and the results are shown in fig. 12. Where the pressure drop, Nusselt number, and FOM value corresponding to the optimal solution are all represented by symbols ★ in fig. 12, while the heat transfer coefficient and Reynolds number corresponding to the optimal solution are represented by symbols ▲ in the figures.

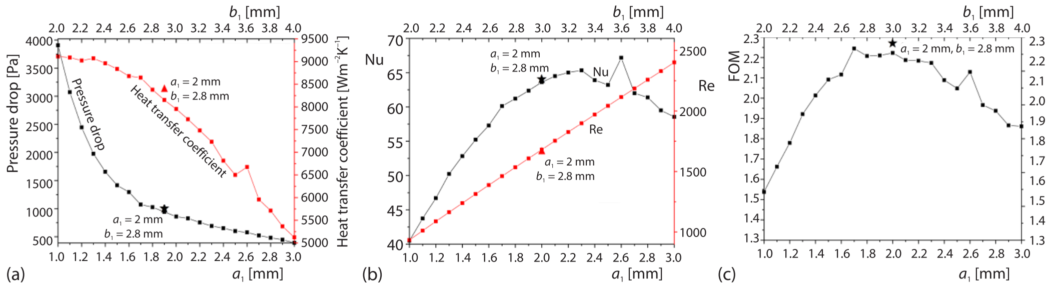

Figure 12. Comparison of structural performance parameters of cooling plate with 6 channel ellipse section obtained by BOBYQA algorithm; (a) pressure drop and heat transfer coefficient, (b) Nusselt and Reynolds numbers, and (c) FOM

Through figs. 12(a) and 12(b), it can be found that the pressure drop and heat transfer coefficient corresponding to the optimal solution obtained after optimization by the BOBYQA algorithm are close to the parametric scan results, and the Nusselt and Reynolds numbers are slightly larger than the optimal solutions corresponding to the parametric scan. In fig. 12(c), it can be summarized that using the BOBYQA algorithm can obtain better FOM values than the parametric. The optimal solution (a_1 = 2 mm, b_1 = 2.8 mm) is close to that of the parametric scan (a_1 = 2 mm, b_1 = 3 mm), which further shows that the optimization by BOBYQA algorithm is effective. Table 7 shows the comparison between the unoptimized model, the optimized model and the results of [7]. For the optimized model, it can be seen from tab. 7 that the pressure drop is reduced by 85.37% and the heat transfer coefficient is increased by 33.03% compared with the results of [7].

Table 7. The comparison between the unoptimized model, the optimized model and an already published work

	[7]	Unoptimized model	Optimized model
Pressure drop [Pa]	5942	859.63	896.3
Pump power [W]	0.048135	0.00928	0.00968
Heat transfer coefficient [Wm^{-2}K^{-1}]	6192.3	7952.3	8237.4
FOM	1	2.223	2.271

Conclusions

In this paper, the heat dissipation capacity of the cooling plate of permanent magnet LSM based on multiple channels is proposed, and compared with the reported Baseline cooling channel. Secondly, the optimization design based on heat dissipation capacity and pumping power is carried out. The research conclusions are as follows.

- Multiple channels can effectively improve the heat dissipation capacity compared with the traditional cooling channel. In this paper, the heat dissipation capacity can reach optimum when the channel number is 6.
- Compared and analyzed the heat dissipation capacity of the cooling plate with five section shapes, among which rectangle section and ellipse section can achieve better cooling effect.

- The BOBYQA algorithm is used to find the optimal solution of section sizes. Obtained optimized scheme (a_1 = 2 mm, b_1 = 2.8 mm) reduces the pressure drop by 85.37% and improve heat transfer coefficient by 33.03% compared with original cooling plate, which realizes a trade-off with heat transfer coefficient and pump power.

Nomenclature

P_{Cu} – total copper loss, [W]
q_w – heat flux, [Wcm^{-2}]
Re – Reynolds number, [–]
Nu – Nusselt number, [–]
h_m – heat transfer coefficient, [Wm^{-2}K^{-1}]

Greek symbol

Ω – pressure drop, [Pa]

Acronyms

BOBYQA – Boundary optimization by quadratic approximation
LSM – linear synchronous motor

References

[1] Boldea, I., *et al*., Linear Electric Machines, Drives and MAGLEVs: an Overview, IEEE Transactions on *Industrial Electronics*, *65* (2018), 9, pp. 7504-7515
[2] Elwell, R. J., *et a*l., Thermal Management Techniques for an Advanced Linear Motor in an Electric Aircraft Recovery System, *IEEE Transactions on Magnetics*, *37* (2001), 1, pp. 476-479
[3] Chai, F., *et al*., Temperature Field Accurate Modelling and Cooling Performance Evaluation of Direct-Drive Outer-Rotor Air-Cooling In-Wheel Motor, *Energies*, *9* (2016), 818
[4] Park, J., *et al.*, Enhancement of Cooling Performance in Traction Motor of Electric Vehicle Using Direct Slot Cooling Method, *Applied Thermal Engineering*, *217* (2022), 119082
[5] Ha, T., *et al*., Experimental Study on Behavior of Coolants, Particularly the Oil-Cooling Method, in Electric Vehicle Motors Using Hairpin Winding, *Energies*, *14* (2021), 956
[6] Jang, C., *et al*., Heat Transfer Analysis and Simplified Thermal Resistance Modelling of Linear Motor Driven Stages for SMT Applications, *IEEE Transactions on Components and Packaging Technologies*, *26* (2003), 3, pp. 532-540
[7] Pei, Z., *et al*., Temperature Field Calculation and Water-Cooling Structure Design of Coreless Permanent Magnet Synchronous Linear Motor, *IEEE Transactions on Industrial Electronics*, *68* (2021), 2, pp. 1065-1076
[8] Pan, D., *et al*., Modelling and Optimization of Air-Core Monopole Linear Motor Based on Multiphysical Fields, *IEEE Transactions on Industrial Electronics*, *65* (2018), 12, pp. 9814-9824
[9] Lu, Q., *et al*., Modelling and Investigation of Thermal Characteristics of a Water-Cooled Permanent-Magnet Linear Motor, *IEEE Transactions on Industry Applications*, *51* (2015), 3, pp. 2086-2096
[10] Xi, L., *et al*., Study on Flow and Heat Transfer Characteristics of Cooling Channel Flied with X-Shaped Truss Array, *Thermal Science*, *27* (2022), 1B, pp. 739-754
[11] Zehforoosh, A., *et al*., Numerical Investigation of Pressure Drop Reduction Without Surrendering Heat Transfer Enhancement in Partially Porous Channel, *International Journal of Thermal Sciences*, *49* (2010), pp. 1649-1662
[12] Hajmohammadi, M. R., *et al*., Thermal Performance Improvement of Micro-Channel Heat Sinks by Utilizing Variable Cross-Section Micro-Channels Filled with Porous Media, *International Communications in Heat and Mass Transfer*, *126* (2021), 105360
[13] Lu, S., *et al*., A Comparative Analysis of Innovative Micro-Channel Heat Sinks for Electronic Cooling, *International Communications in Heat and Mass Transfer*, *76* (2016), Aug., pp. 271-284
[14] Hung, T. C., et al., Thermal Performance Analysis of Porous Micro-Channel Heat Sinks with Different Configuration Designs, *International Journal of Heat and Mass Transfer*, *66* (2013), Nov., pp. 235-243
[15] Powell, M. J. D., The BOBYQA Algorithm for Bound Constrained Optimization without Derivatives, Report DAMTP 2009/NA06, Cambridge, UK, 2009, pp. 26-46

Paper submitted: November 11, 2022
Paper revised: December 19, 2022
Paper accepted: December 26, 2022